Physics – Uspekhi **55** (9) 929 – 941 (2012)

CONFERENCES AND SYMPOSIA PACS numbers: 01.10.Fv, **26.60. – c**, **52.35. – g**, **67.10. – j**, **96.60. – j**, 97.10.Sj, 97.60.Jd

Challenges in astrophysics
(Scientific session of the Physical Sciences Division of the Russian Academy of Sciences, 25 January 2012)

DOI: 10.3367/UFNe.0182.201209e.0999

On 25 January 2012, the scientific session of the Physical Sciences Division of the Russian Academy of Sciences (RAS), entitled as ''Challenges in astrophysics'', was held at the conference hall of the Lebedev Physical Institute, RAS.

The following reports were put on the session agenda posted on the website www.gpad.ac.ru of the RAS Physical Sciences Division:

(1) **Stepanov A V** (Central (Pulkovo) Astronomical Observatory, RAS, St. Petersburg) ''Coronal seismology'';

(2) **Yakovlev D G** (Ioffe Physical Technical Institute, St. Petersburg; St. Petersburg State Polytechnical University, St. Petersburg) ''Superfluid neutron stars''.

The papers written on the base of the oral reports are published below.

PACS numbers: **52.35. – g**, **96.60. – j**, 97.10.Sj
DOI: 10.3367/UFNe.0182.201209f.0999

Coronal seismology

A V Stepanov, V V Zaitsev, V M Nakariakov

1. Introduction

Coronal seismology is a new, rapidly developing branch of astrophysics studying wave and oscillatory phenomena intrinsic to coronae of active stars. The idea of coronal seismology is reminiscent of that of *geoseismology* and lies in the remote sensing of coronal plasma parameters. In solar and stellar physics, a similar approach is applied in *helio-* and *asteroseismology*. Present-day observations of waves and oscillations in accretion disks led to the appearance of *diskoseismology*.

The task of helioseismology consists in testing and perfecting the model of the Sun. Among its achievements is the confirmation of the 'standard' Sun model and the creation of the shallow sunspot model [1]. Newly emerging tasks of helioseismology are being solved with the help of the operating NASA's Solar Dynamic Observatory (SDO) mission [2]. The main tasks of asteroseismology concern the verification and improvement of existing evolutionary models of stars.

The founders of *coronal seismology* are Y Uchida [3], who proposed exploring the plasma of the Sun's corona with the help of oscillations and waves, and H Rosenberg [4], who explained pulsations in solar radio-frequency emission by magnetohydrodynamic (MHD) oscillations in its source. Observations of solar ultraviolet (UV) emission in space by the NASA's TRACE (Transition Region and Coronal Explorer) mission revealed oscillations of coronal loops [5] (Fig. 1), which gave impetus to the fast development of coronal seismology.

The magnetic structure of the coronae of the Sun and other stars includes both open and closed configurations (magnetic tubes). Solar spicules, jets, and streamers are the examples of open configurations. Among the closed configurations are flaring active regions consisting of a system of loops, seldom of a single loop flare. Flare loops make up magnetic traps for accelerated particles. MHD oscillations of loops are accompanied by variations in the magnetic field and gas pressure, as well as by the modulation of high-energy particle fluxes to the loop footpoints. For this reason, the flare emission is modulated in a broad band, including radio, optical, X-ray, and gamma ranges. Characteristics of these modulations are used to diagnose flare parameters.

Two approaches are routinely used to describe wave and oscillatory phenomena in stellar coronae. In the first one, coronal magnetic loops and tubes are considered as resonators and waveguides for MHD oscillations and waves. In the second approach, the coronal magnetic loop is viewed as an electric current circuit. Both approaches are indispensable for diagnosing physical processes in stellar coronae.

2. Coronal resonators and waveguides

The impedance for MHD waves experiences a jump at the boundary between coronal loops and the ambient medium; hence, a coronal loop can be conceived of as a resonator. In the first approximation, loop oscillations can be explored by considering a homogeneous plasma cylinder of radius a and length l, the ends of which are frozen in a highly conductive plasma. The plasma inside the cylinder has the density ρ_i, temperature T_i, and magnetic field induction B_i along the cylinder axis. The respective parameters outside the cylinder are ρ_e, T_e, and B_e. The dispersion relation connecting the

A V Stepanov Central (Pulkovo) Astronomical Observatory, Russian Academy of Sciences, St. Petersburg, Russian Federation
E-mail: stepanov@gao.spb.ru
V V Zaitsev Institute of Applied Physics, Russian Academy of Sciences, Nizhny Novgorod, Russian Federation
E-mail: za130@appl.sci-nnov.ru
V M Nakariakov Centre for Fusion, Space, and Astrophysics, Physics Department, University of Warwick, Coventry CV4 7AL, UK
E-mail: V.Nakariakov@warwick.ac.uk

Uspekhi Fizicheskikh Nauk **182** (9) 999 – 1012 (2012)
DOI: 10.3367/UFNr.0182.201209e.0999
Translated by S D Danilov, D G Yakovlev; edited by A Radzig

Uspekhi Fizicheskikh Nauk **182** (9) 999 – 1005 (2012)
DOI: 10.3367/UFNr.0182.201209f.0999
Translated by S D Danilov; edited by A Radzig

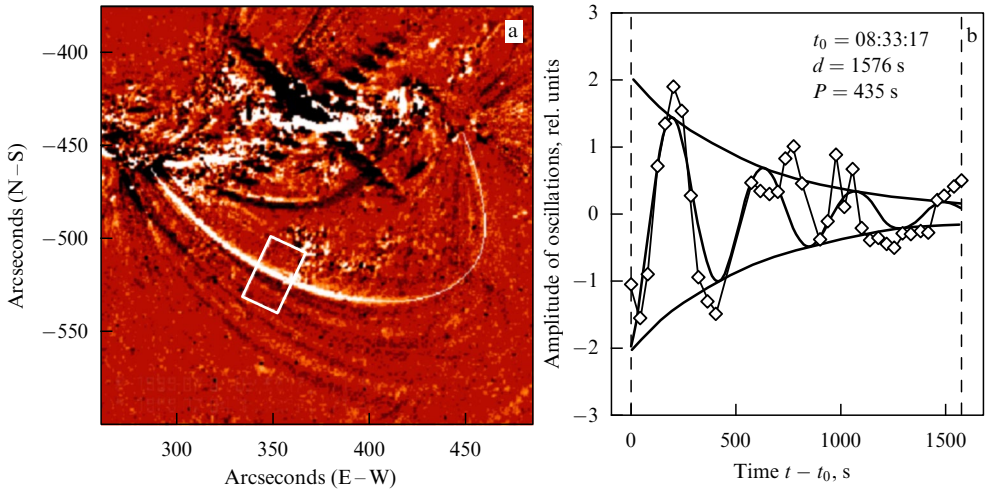

Figure 1. (a) An example of oscillations of the coronal loop for the flare on July 4, 1999, recorded by space mission TRACE in the 171 Å line. (b) Their approximation by exponentially decaying periodic oscillations. The period of pulsations $P = 435$ s, their duration $d = 1576$ s, and their amplitude was on the order of 700 km [5].

frequency ω of natural oscillations of the cylinder with the wave vector components $k_\perp$ and $k_\parallel$ takes the form [6, 7]

$$\frac{J'_m(\kappa_i a)}{J_m(\kappa_i a)} = \alpha \frac{H_m^{(1)'}(\kappa_e a)}{H_m^{(1)}(\kappa_e a)} . \qquad (1)$$

Here, the following notations were introduced:

$$\kappa^2 = \frac{\omega^4}{\omega^2(c_s^2 + c_A^2) - k_\parallel^2 c_s^2 c_A^2} - k_\parallel^2 , \qquad \alpha = \frac{\kappa_e \rho_i}{\kappa_i \rho_e} \frac{\omega^2 - k_\parallel^2 c_{Ai}^2}{\omega^2 - k_\parallel^2 c_{Ae}^2} ,$$

c_s is the speed of sound, c_A is the Alfvén speed, J_m and $H_m^{(1)}$ are the Bessel function and the Hankel function of the first kind, respectively, and $k_\parallel = \pi s/l$, $s = 1, 2, 3, \ldots$. For a thin $(a/l \ll 1)$ and dense $(\rho_e/\rho_i \ll 1)$ cylinder, we find the frequency of fast (FMA) and slow (SMA) magneto-acoustic oscillations from Eqn (1) at $m = 0$:

$$\omega_f = (k_\perp^2 + k_\parallel^2)^{1/2}(c_{si}^2 + c_{Ai}^2)^{1/2} , \qquad \omega_s = \frac{k_\parallel c_{si} c_{Ai}}{(c_{si}^2 + c_{Ai}^2)^{1/2}} . \qquad (2)$$

The transverse wave number $k_\perp = \lambda_j/a$, where λ_j are the zeros of the Bessel function $J_0(\lambda) = 0$.

Radial FMA oscillations (the sausage mode), contributing most to the modulation of loop emission, may experience substantial damping due to their emission into the surrounding medium [8]:

$$\gamma_a = \frac{\pi}{2} \omega_f \left(\frac{\rho_e}{\rho_i} - \frac{k_\parallel^2}{k_\perp^2} \right) , \qquad \frac{\rho_e}{\rho_i} > \frac{k_\parallel^2}{k_\perp^2} . \qquad (3)$$

The mechanism for acoustic damping is apparent: loop oscillations are accompanied by the excitation of waves in the surrounding medium, which requires the oscillation energy expenditure. The acoustic damping is absent for $\rho_e/\rho_i < k_\parallel^2/k_\perp^2$, which corresponds to total internal reflection, i.e., a 'thick' loop with $l/a < 1{,}3(\rho_i/\rho_e)^{1/2}$ is an ideal resonator for FMA waves. Oscillations in the global FMA mode were observed in the solar flare on January 12, 2000, recorded at a frequency of 17 GHz by Radioheliograph Nobeyama [9]. In this case, all regions of the flare loop were oscillating in phase with the period $P \approx l/c_{Ai} \approx 15$ s.

The case of $m = 1$ corresponds to kink loop oscillations (see Fig. 1) which were observed for the first time by TRACE. For $k_\parallel a \ll 1$ and $B_e \approx B_i$, equation (1) yields the kink mode frequency [10]

$$\omega_k \approx k_\parallel \left(\frac{2}{1 + \rho_e/\rho_i} \right)^{1/2} c_{Ai} . \qquad (4)$$

In the event on July 4, 1999 (see Fig. 1), the phase velocity of kink mode approached to $\omega/k_\parallel = 2l/P \approx 1000$ km s^{-1}. Taking into account relation (4) and assuming $\rho_e/\rho_i = 0.1$ in the interval $10^9 - 10^{10}$ cm^{-3} of electron density in the loop, we estimate the magnetic field intensity:

$$B_i = \sqrt{2\pi} \frac{2l}{P} \sqrt{\rho_i \left(1 + \frac{\rho_e}{\rho_i} \right)} \approx 10 - 33 \text{ G} .$$

A numerical solution of the transcendent equation (1) with a complex frequency of oscillations $\omega = \omega_0 - i\gamma$, where γ is the decrement, is plotted in Fig. 2 which shows the dependences of $\omega_0/k_\parallel$ and $\gamma/k_\parallel$ on $k_\parallel a = s\pi a/l$ for the first three harmonics of FMA oscillations [11].

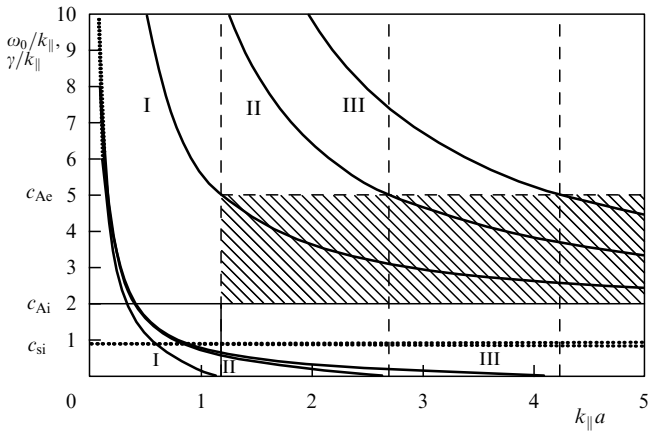

Figure 2. Dispersion curves and decrements of acoustic damping for the first three harmonics of FMA oscillations at $c_{se} = 0.5c_{si}$, $c_{Ai} = 2c_{si}$, and $c_{Ae} = 5c_{si}$ [11].

To compare the results of Ref. [11] to those obtained by Edwin and Roberts [7] for trapped modes, the same relationships as in the latter work have been used for velocities in the solar corona. The dispersion curves in the domain of trapped modes in the interval $c_{Ai} < \omega_0/k_\parallel < c_{Ae}$ (the dashed area in Fig. 2) coincide with those in Ref. [7] and have a natural continuation for $\omega_0/k_\parallel > c_{Ae}$. It was assumed in Ref. [7] that $\kappa_e^2 < 0$, i.e., the arguments of cylindrical functions were taken as imaginary. In this case, the solution of Eqn (1) in the outer domain is expressed in terms of the Mcdonald function $K_m(z) = (\pi/2)\mathrm{i}^{m+1}H_m^{(1)}(\mathrm{i}z)$, i.e., the solution of equation (1) includes nonleaky modes as a particular case for the imaginary $\kappa_e a$. Note that the nonleaky sausage modes occur only for 'thick' loops: $k_\parallel a = s\pi a/l > 1$. In coronae of the Sun (see Fig. 1) and stars the loops are thin: $k_\parallel a < 1$, i.e., the MHD modes are emitting. Simultaneously, the period of FMA oscillations is determined not by the length of the loop, but by its radius:

$$P_f = \frac{2\pi a}{\lambda_j\sqrt{c_{Ai}^2 + c_{si}^2}}\,. \qquad (5)$$

Figure 2 also depicts the branches of the SMA mode $\omega_s = k_\parallel c_{si}$, and the Alfvén mode $\omega_A = k_\parallel c_{Ai}$. Accounting for curvature of the magnetic field in coronal loops is important for the ballooning mode of the flute type instability [12].

In addition to oscillations, one can observe propagating waves (Fig. 3) in coronal loops. The TRACE observations revealed longitudinal compressive waves of a small amplitude (4–10%) with periods of 3–12 min and a mean propagation speed of ≈ 100 km s^{-1} [13]. This interval of periods also includes five-minute photospheric oscillations. The energy flux in these waves of ≈ 0.3 W m^{-2} is, however, substantially lower than the level of order 100 W m^{-2} needed to heat the solar corona to a temperature of 10^6 K.

Incompressible Alfvén type waves are more efficient in carrying the energy of convective motions in stellar photospheres to coronae than are magneto-acoustic waves. It was believed earlier that the amplitudes of Alfvén waves in the solar corona do not exceed 0.5 km s^{-1}, i.e., that their energy flux is insufficient to heat the corona. Recent SDO data [14] have shown that the amplitudes may reach 20 km s^{-1}, i.e., the energy of kink (Alfvénic) waves may suffice to heat the solar corona and accelerate the solar wind. The main problem consists in elucidating the mechanism for kink (Alfvénic) wave dissipation.

MHD modes in X-ray jets and spicules are described with the model of a plasma cylinder with one end fixed [15].

3. Mechanisms of excitation and damping of magnetohydrodynamic oscillations

An often encountered mechanism for the generation of loop oscillations consists in their excitation by an external source, which can be a flare, filament eruption, or electrodynamically coupled neighboring loop-trigger [16]. If flare energy release happens inside a coronal loop, then, given that the flare has a sufficiently fast (impulse) character, the generation of FMA loop oscillations becomes possible [17]. The FMA modes of loops can also be excited by high-energy protons at bounce resonance, $\omega_f = s\Omega$, $s = 1, 2, 3, \ldots$, where Ω is the frequency of oscillations for high-energy protons between magnetic mirrors of the coronal loop. In this case, the pressure of protons trapped in the loop should be fairly high: $\beta_{pr} > 0.2$ [8].

The kink mode (4) can be generated during solar flares and also because of the evaporation of hot ($\geqslant 10^7$ K), dense chromospheric plasma from loop footpoints [18]. The motion of the chromospheric matter at the speed $V \geqslant 3 \times 10^7$ cm s^{-1} along the magnetic field in a loop with the curvature radius R causes the centrifugal force $F_c = \rho V^2/R$ 'stretching' the loop. The tension of magnetic field lines tends to return the loop to its initial state, which results in the excitation of loop oscillations with the period $P_k = 2\pi/\omega_k$. The excitation of loops due to the parametric resonance with acoustic five-minute oscillations of the Sun's photosphere is considered in Section 6.

The Q factor for oscillations in solar and stellar flares is, as a rule, not very high: $Q = \pi\omega/\gamma = 10-30$. Modes without leakage decay because of dissipative processes inside the loops. This, with the exception of special cases, is related to emitting modes, too. The point is that the loop–ambient plasma interface is characterized by an impedance jump for MHD waves and the possible ratio of intensities of incident and reflected waves, $I_{ref}/I_{inc} = (Z_i - Z_e)^2/(Z_i + Z_e)^2$, being close to unity. The impedance for FMA waves is defined as $Z = \rho(c_A^2 + c_s^2)^{1/2}$. If, for example, the ratio $\rho_i/\rho_e \approx 30-100$ and $\beta = 8\pi n k_B T/B^2 \approx (c_s/c_A)^2 \ll 1$, then $I_{ref} \approx I_{inc}$. The total decay decrement for FMA waves, $\gamma_\Sigma = \gamma_J + \gamma_{cond} + \gamma_\nu + \gamma_{rad}$, contains contributions due to Joule dissipation, electron heat conductivity, ion viscosity, and radiation loss [19]:

$$\gamma_J = \frac{1}{2}\frac{m_e}{m_i}\frac{\omega^2}{\omega_i^2}\nu_{ei}\,, \qquad \gamma_{cond} = \frac{1}{3}\frac{m_e}{m_i}\beta^2\frac{\omega^2}{\nu_{ei}}\sin^2\vartheta\cos^2\vartheta\,,$$
$$\gamma_\nu = \frac{1}{12}\sqrt{\frac{m_i}{2m_e}}\left(\frac{V_{Ti}}{c_A}\right)^2\frac{\omega^2}{\nu_{ei}}\sin^2\vartheta\,, \quad \gamma_{rad} = \frac{2\pi}{3}\frac{n^2\phi(T)}{B^2}\sin^2\vartheta\,. \qquad (6)$$

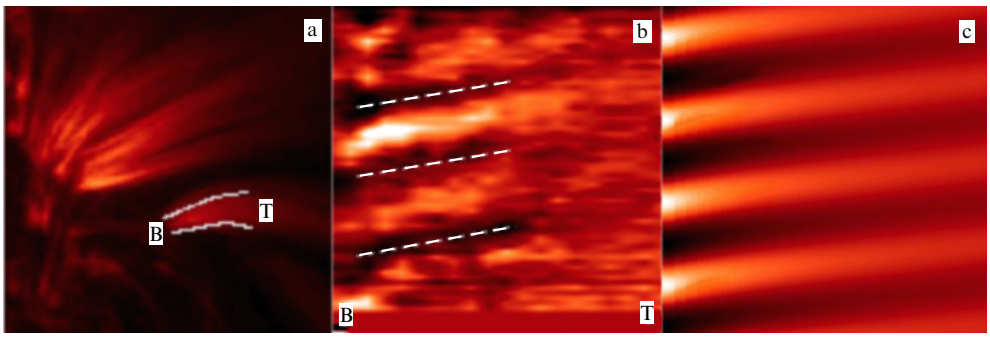

Figure 3. (a) An example of waves propagating from the footpoints of the loop structure as observed by TRACE (171 Å) on April 7, 2000. (b) Time–distance diagram revealing propagating waves. (c) Results of numerical simulations of the propagating perturbation [13].

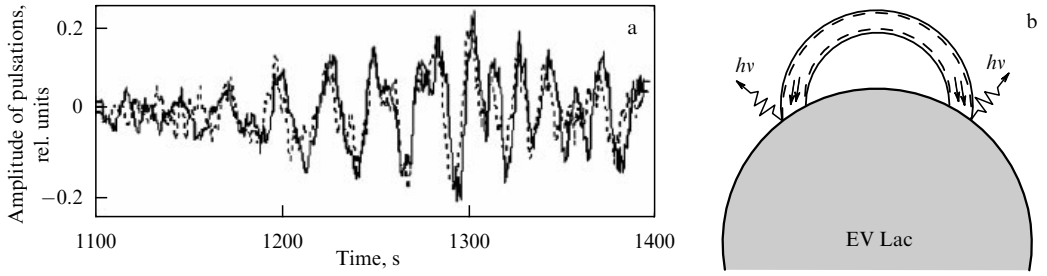

Figure 4. (a) Oscillations of the emission from a flare on EV Lac on 11.09.1998 in the bands U (solid line) and B (dashed line) with the period $P \approx 13$ s [20]. (b) Schematic representation of optical emission pulsations [21].

Here, ϑ is the angle between **B** and the wave vector **k**, ω_i is the ion gyrofrequency, $\nu_{ei} \approx 60nT^{-3/2}\ \mathrm{s}^{-1}$, and $\phi(T) = 5 \times 10^{-20} T^{-1/2}$ is the loss function for the temperature interval $10^6 < T < 10^7$ K [20]. In coronae of the Sun and stars of the UV Ceti type (active red dwarfs) the major contributions to the decay of FMA waves come from electron heat conductivity (γ_{cond}) and ion viscosity (γ_ν). In stellar chromospheres, the main cause of damping is the radiation losses (γ_{rad}).

4. Diagnostics of flare loop parameters

The hypothesis of modulation of the emission from solar and stellar flares with MHD oscillations of loops is successfully invoked to diagnose flare plasmas. In stellar coronae, loop oscillations modulate radio-frequency emission, while in the chromosphere and photosphere they modulate optical, X-ray, and gamma radiations caused by intrusions of high-energy particles in dense footpoints of flare loops. The intensity of emission from the footpoints is proportional to the flux of 'precipitating' accelerated particles, $F \sim l n_1 / \sigma t_D(\sigma)$. Here, n_1 is the number density of high-energy particles, $\sigma = B_{max}/B_{min}$ is the mirror ratio of the loop, and $t_D(\sigma)$ is the pitch-angular particle diffusion time into the loss cone, which depends on the diffusion mode. Relative variations of emitted flux are proportional to the variations of the mirror ratio caused by magnetic field oscillations, i.e., $\delta F/F \approx \delta\sigma/\sigma \approx \delta B/B$. To find δB, we assume that the generation of FMA oscillations proceeds at the expense of the work done by plasma pressure against the loop magnetic field during pulse heating, $\delta p \approx n k_B T$. Consequently, $\delta B/B \approx 4\pi n k_B T/B^2$ and the emission modulation depth is given by [17]

$$\Delta = \frac{\delta F}{F} \approx \frac{4\pi n k_B T}{B^2} = \frac{\beta}{2}\,. \tag{7}$$

From the three equations for the period of FMA oscillations (5) at $\lambda_0 = 2.4$, Q factor $Q = \pi\omega/(\gamma_{cond} + \gamma_\nu)$, and the emission modulation depth (7) we obtain the formulas to determine the parameters of the flare plasma:

$$\begin{aligned} T &\approx 1.2 \times 10^{-8}\, \frac{\tilde{r}^2 \Delta}{P^2 \chi}\ [\mathrm{K}]\,, \\ n &\approx 3.5 \times 10^{-13}\, \frac{\tilde{r}^3 \eta \Delta^{5/2} Q \sin^2\vartheta}{P^4 \chi^{3/2}}\ [\mathrm{cm}^{-3}]\,, \\ B &\approx 3.8 \times 10^{-18}\, \frac{Q^{1/2} \tilde{r}^{5/2} \eta^{1/2} \Delta^{5/4} \sin\vartheta}{P^3 \chi^{5/4}}\ [\mathrm{G}]\,, \end{aligned} \tag{8}$$

where $\tilde{r} = 2\pi a/\lambda_0$, $\eta = 243\beta\cos^2\vartheta + 1$, $\chi = 10\Delta/3 + 1$, and $\vartheta = \arctan(k_\perp/k_\parallel) \approx \arctan(l/a)$.

Let us consider the examples of such diagnostics. Pulsations in the flare on EV Lac 11.09.98 (Fig. 4) were observed in the ultraviolet (UV) and blue (B) bands with a period $P \approx 13$ s, the Q factor ≈ 50, and $\Delta \approx 0.2$ [21]. Setting $a/l = 0.1$, i.e., $\vartheta \approx \arctan(\lambda_0 l/\pi a) \approx 76°$, and assuming $\tilde{r} = 2.62a \approx 2.62 \times 10^9$ cm, from formulas (8) we find $T \approx 3.7 \times 10^7$ K, $n \approx 1.6 \times 10^{11}\ \mathrm{cm}^{-3}$, and $B \approx 320$ G.

For pulsations of the optical emission in the flare on EQPegB (M5e) with a period of about 10 s, the Q factor ≈ 30, and $\Delta \approx 0.1$, from formula (8) we get $T \approx 6 \times 10^7$ K, $n \approx 3 \times 10^{11}\ \mathrm{cm}^{-3}$, and $B \approx 540$ G [22].

A popular method of diagnosing parameters of stellar coronae [23] is based on the assumption that, on plasma cooling, the radiation losses are on the order of losses due to electron heat conductivity: $\gamma_{rad} \approx \gamma_{cond} \approx 1/\tau_d$. Then, based on measurements of the emission measure (EM) and flare decay time τ_d, the temperature, number density, and size of the emitting domain can be determined as:

$$\begin{aligned} T\,[\mathrm{K}] &= 4 \times 10^{-5} (\mathrm{EM})^{0.25} \tau_d^{-0.25}\,, \\ n\,[\mathrm{cm}^{-3}] &= 10^9 (\mathrm{EM})^{0.125} \tau_d^{-0.125}\,, \\ l\,[\mathrm{cm}] &= 5 \times 10^{-6} (\mathrm{EM})^{0.25} \tau_d^{0.75}\,, \end{aligned}$$

and the magnetic field can be estimated from the relationship $\beta < 1$. Our approach allows the estimation of three fundamental parameters, T, n, and B, from the pulsation period, Q factor, and emission modulation depth. Both approaches expand the possibilities of stellar corona diagnostics.

Microwave flare emission is frequently caused by gyrosynchrotron emission of high-energy electrons with a power-law energy spectrum $N(E) \propto E^{-\alpha}$. In this case, the intensity of emission from optically thin and optically thick sources is written down in the form

$$I_\nu \propto \begin{cases} B^{0.9\alpha - 0.22}\,, & \tau_\nu \ll 1\,, \\ B^{-0.52 - 0.08\alpha}\,, & \tau_\nu \gg 1\,. \end{cases} \tag{9}$$

It can easily be seen that the emission of an optically thin source is rather sensitive to magnetic field variations. Moreover, from Eqn (9) it follows that, given appropriate values for α, pulsations of the emission from optically thin and thick sources will be in antiphase, as was observed for the solar flare on May 31, 1990, recorded at frequencies of 9 GHz ($\tau_\nu \gg 1$) and 15 GHz ($\tau_\nu \ll 1$) [24]. The modulation depths for optically thin and thick sources are equal, respectively, to

$$\begin{aligned} \Delta_1(\tau_\nu < 1) &= 2(0.9\alpha - 1.22)\, \frac{\delta B}{B}\,, \\ \Delta_2(\tau_\nu > 1) &= 2(0.08\alpha + 1.02)\, \frac{\delta B}{B}\,. \end{aligned}$$

Thus, one has

$$\alpha = \frac{1.22 + 1.02(\Delta_1/\Delta_2)}{0.9 - 0.08(\Delta_1/\Delta_2)} . \quad (10)$$

For the above-mentioned event, $\Delta_1 = 5\%$, and $\Delta_2 = 2.5\%$. From expression (10) we obtain $\alpha = 4.4$ for the power-law exponent of the high-energy (> 30 keV) electron spectrum. From formulas for gyrosynchrotron emission, one determines the magnetic field induction in the source: $B \approx 150$ G [25].

5. Coronal magnetic loops as equivalent electric (*RLC*) circuits

One of the important problems of coronal physics pertains to diagnosing electric currents. The current in radio source 3C 228 ($I \approx 2.5 \times 10^9$ A) was determined through the rotation of the radiation polarization ellipse (the Faraday effect) [26]. A Severny [27] was the first to estimate the magnitude of current ($I \geqslant 10^{11}$ A) in the vicinity of solar spots based on magnitographic measurements. Based on the measurements by Severny, H Alfvén proposed describing the flare loop in terms of a wire carrying electric current. The Alfvén model [28] gained attention owing to flare loop observations by cosmic solar observatories. The model of the flare as an equivalent electric circuit is described in review [29].

Examples of magnetic tube formation by converging streams of photospheric plasma are given in Fig. 5. There are oppositely directed convective flows across the boundaries separating supergranules, and an extended layer of the magnetic field with relatively substantial strength (Fig. 5a) may appear along the boundaries.

A Rayleigh–Taylor type interchange instability may occur in this layer. As a result, it breaks into a system of magnetic tubes with a radius on the order of the layer thickness (Fig. 5b), which may form an arcade of coronal magnetic loops in the corona. If a magnetic tube made up at a contact point of more than two cells, the converging flow of photospheric plasma forms a compact cylindrical magnetic tube with current from the background magnetic field (Fig. 5c). Indeed, the electron gyrofrequency in the upper photosphere is higher than the effective frequency of electron–atom collisions, $\omega_e \gg \nu'_{ea}$, and the gyrofrequency of ions is lower than the frequency of ion–atom collisions, $\omega_i \ll \nu'_{ia}$. The electrons are, consequently, magnetized, and the ions are entrained by the neutral plasma component, which leads to the emergence of the radial electric field E_r of charge separation. Field E_r, together with the primary magnetic field B_z, generates the Hall current j_φ which amplifies the primary field B_z. The amplification of the magnetic field continues until 'raking' of the background magnetic field is compensated for by magnetic field diffusion. A magnetic tube forms as a result, the magnetic field of which is determined by the energy deposition of the convective plasma flow for the tube formation time of order R_0/V_r, where $R_0 \sim 30{,}000$ km is the scale of the supergranulation cell, and $V_r \sim 0.1$–0.5 km s^{-1} is the horizontal velocity of convective motion.

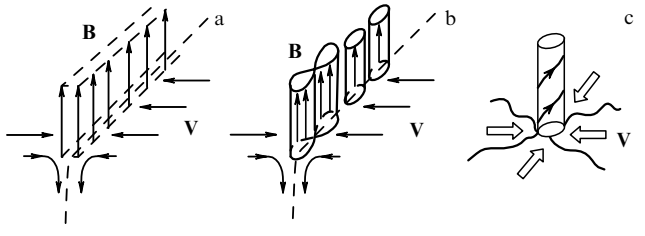

Figure 5. Formation of magnetic field tubes at the boundaries of supergranulation cells: (a) the build-up of the extended thin magnetic layer; (b) breakup of the layer into magnetic tubes as a result of interchange instability, and (c) formation of a magnetic tube in a node of several supergranulation cells.

In the coronal part of the loop, the plasma parameter $\beta \ll 1$ and the loop structure is forceless, i.e., the electric current lines are directed nearly along the magnetic field lines. The current is closed in the subphotospheric domain where the plasma conductivity is isotropic and the current follows the shortest path from one loop footpoint to the other one.

The equation for small-amplitude current oscillations $|\tilde{I}| \ll I$ has the form [30]

$$\frac{L}{c^2}\frac{\mathrm{d}^2\tilde{I}}{\mathrm{d}t^2} + \left[R(I) - \frac{|V_r|l}{ac^2}\right]\frac{\mathrm{d}\tilde{I}}{\mathrm{d}t} + \frac{\tilde{I}}{C(I)} = 0 . \quad (11)$$

Here, the notations are as follows:

$$R(I) \approx \frac{4I^2 l\xi^2}{c^4 n m_i \nu'_{ia}\pi a^4} , \qquad C(I) \approx \frac{c^4 n m_i S^2}{2\pi l I^2} ,$$
$$L = 2l\Lambda , \qquad \Lambda \approx \ln\frac{4l}{\pi a} - \frac{7}{4} , \quad (12)$$

where $\xi = \rho_a/\rho$ is the relative number density of neutral particles, and S is the loop cross-section area. From equation (11) it follows that oscillations in the circuit build up if $R(I) < |V_r|l/ac^2$, i.e., if the current in the circuit is less than the stationary value, and decay if the photospheric electromotive force (EMF) ceases to act. In this case, the decay is rather slow, since the Q factor of the circuit is high: $Q = [cR(I)]^{-1} \times \sqrt{LC(I)} \sim 10^3 - 10^4$ for typical flare loops. From relationships (12) it follows that the frequency of flare-loop *RLC* oscillations for a strong enough current is proportional to its magnitude [29]:

$$\nu_{RLC} = \frac{c}{2\pi\sqrt{LC(I)}} \approx \frac{1}{(2\pi)^{3/2}\Lambda^{1/2}}\frac{I}{ca^2\sqrt{\rho}} \approx \frac{B_\varphi}{2\pi a\sqrt{4\pi\rho}} . \quad (13)$$

The condition that oscillations be in phase requires that relationships for the Alfvén time $\tau_A = l/c_A < T_{RLC} = 1/\nu_{RLC}$ be satisfied. Since $I \approx caB_\varphi/2$, the twisting of the loop magnetic field should be small, $B_\varphi/B_z < \pi\sqrt{2\Lambda}\,(a/l)$, which is observed for solar loops. Formula (13) corresponds to Alfvén oscillations of the coronal magnetic loop with the wave vector of absolute value $|\mathbf{k}| \approx a^{-1}$ directed at the angle $\cos\theta \approx (B_\varphi/B_z)$ to the magnetic field. In this case, one obtains

$$\nu_A = \frac{1}{2\pi} kc_A \cos\theta \approx \frac{1}{2\pi a}\frac{\sqrt{B_z^2 + B_\varphi^2}}{\sqrt{4\pi\rho}}\frac{B_\varphi}{B_z} ,$$

i.e., the frequency of Alfvén oscillations coincides with that in formula (13) since $B_\varphi \ll B_z$.

Formula (13) is applied to diagnosing electric currents in flares. An example is furnished by the event on March 30, 2001 (Fig. 6) observed by Nobeyama Radio Observatory [31]. Analysis of quasiperiodic pulsations (at frequencies 0.001-0.005 Hz) has revealed an increase in current prior to the flare of up to 10^{10} A, and current dissipation during the

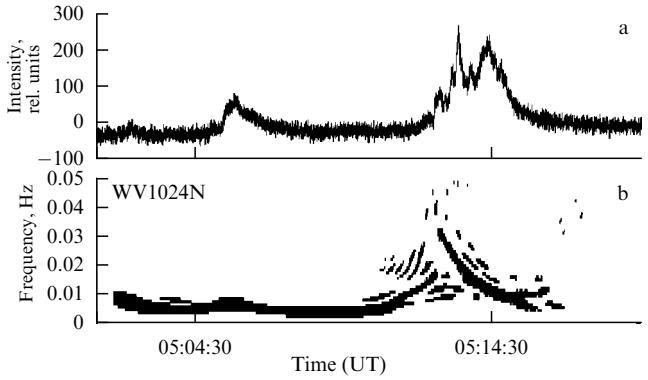

Figure 6. (a) The light curve for the event on 30.03.2001 as observed by spectropolarimeter Nobeyama at a frequency of 17.7 GHz. (b) The spectrum of low-frequency modulation of microwave emission obtained by Wigner–Wille method [32].

flare.

Another example is the solar flare on 24.03.1991 recorded by the Metsähovi Radio Observatory at a frequency of 37 GHz. The current decreased during the flare from 9×10^{11} A to 10^{11} A, the energy stored before the flare amounted to $W = LI^2/2 \sim 10^{32}$ erg, while the energy release power was $\mathrm{d}W/\mathrm{d}t \sim 10^{28}$ erg s^{-1} [29].

6. Parametric resonance

The excitation of acoustic oscillations in coronal magnetic loops may also occur through a parametric resonance with acoustic p-modes [29, 32]. It is known that the frequency of five-minute velocity oscillations of photospheric convection on the Sun (p-modes) is less than the cut-off frequency, i.e., they are reflected from the region of the temperature minimum. However, an analysis of observations of the Sun by the Metsähovi Radio Observatory at a frequency of 11.7 GHz revealed the presence of five-minute oscillations [32]. How do they penetrate into the corona? Moreover, two low-frequency signals with the periods of 3.3 and 10 min have been detected in the spectrum of oscillations, in addition to the signals with the five-minute period. The penetration of p-modes into the corona can be explained by the parametric excitation of acoustic oscillations in the coronal loops. Pulsations of photospheric convection velocity $|V_\mathrm{r}| = V_0 + V_\approx \sin \omega t$ modulate the EMF at the loop footpoints. As a result, the electric current $I_z = I_0 + I_\approx$ flowing in the loop is modulated, too. From the condition of tube radial equilibrium, it follows that the pressure in the tube also varies periodically with the amplitude $p_\approx = 4I_0 I_\approx/3\pi c^2 a^2$. As a result, the speed of sound appears to be periodically modulated:

$$c_\mathrm{s} = \left(\frac{\gamma k_\mathrm{B} T_0}{m_\mathrm{i}}\right)^{1/2}\left(1+\frac{\delta T}{T_0}\right) = c_{\mathrm{s}0}\left(1+\frac{2}{3}\,\frac{\gamma-1}{\gamma}\,\frac{I_0^2}{\pi c^2 a^2 p_0}\,\frac{I_\approx}{I_0}\cos\omega t\right), \qquad (14)$$

and the equation for the longitudinal plasma velocity in acoustic oscillations takes the form of the Mathieu equation, which describes the parametric instability [33]:

$$\frac{\mathrm{d}^2 V_z}{\mathrm{d}t^2} + \omega_0^2(1 + q\cos\omega t)V_z = 0\,, \qquad (15)$$

where the eigenfrequency of acoustic oscillations of the loop $\omega_0 = k_\parallel c_{\mathrm{s}0}$, $k_\parallel = s\pi/l$, $s = 1, 2, 3, \ldots$, $p_0 = 2nk_\mathrm{B}T_0$, $\gamma = c_p/c_v$, and the parameter $q = 4(\gamma-1)I_0 I_\approx/3\gamma\pi c^2 a^2 p_0$. The parametric instability develops in narrow zones near frequencies $\omega_n = n\omega/2$, $n = 1, 2, 3\ldots$. This implies that if the coronal loop is subjected to five-minute photospheric oscillations, acoustic oscillations with periods of 10 min (subharmonic), 5 min (pumping), and 3.3 min (the first upper frequency of parametric resonance) can be excited in the loop. By virtue of this mechanism, the energy of five-minute photospheric pulsations, which are reflected under normal conditions from the temperature minimum, penetrates into the corona, and may serve as an important heating source for the coronal plasma. Estimates in Ref. [34] have shown that heating of the solar corona exceeds radiative cooling, provided the current $I_0 > 7 \times 10^9$ A.

7. Diagnostics of magnetar coronae

One more illustration of the efficiency of methods utilized by coronal seismology is furnished by the diagnostics of coronae of magnetars — neutron stars with a radius of ~ 10 km, mass of $\sim 1.5 M_\odot$, and magnetic field $B \sim 10^{14} - 10^{15}$ G. The energy of the first pulse of an X-ray burst of a magnetar reaches 10^{46} erg [35], which is 14 orders of magnitude higher than the energy of the most powerful solar flares. The first pulse with a duration of about 1 s is followed by a 'pulsating tail' (frequencies from 20 to 2400 Hz) with a duration of about 200–400 s [36]. Existing models are not in the position to explain high Q factors of such pulsations: $Q \approx 10^5 - 10^7$. The magnetar corona comprising a hot plasma trapped by a magnetic field (trapped fireball), to which the pulsating tail is attributed, can be conceived of as a system of magnetic loops of various sizes with their electric current closed by the metallic core of the star [37]. The eigenfrequencies and Q factors of loops are expressed by the relationships $\omega = (LC)^{-1/2}$ and $Q = R^{-1}\sqrt{L/C}$, where $L = 2l\Lambda$ and $C \approx \varepsilon_\mathrm{A} S/l$, and the dielectric constant of the medium for Alfvén waves is $\varepsilon_\mathrm{A} = c^2/c_\mathrm{A}^2 \approx 1$, since from the dispersion relation $\omega_\mathrm{A} = k_\parallel c[1 + (4\pi\rho c^2/B^2)]^{-1/2}$ for Alfvén waves it follows that $c_\mathrm{A} \approx c$ in a magnetar corona.

Take as an example the diagnostics of SGR 1806-20 corona for the flare on December 27, 2004 [37]. The energy in the pulsating tail was on the order of 10^{44} erg. For a 'typical' loop assume that the energy stored in it reaches $\approx 2 \times 10^{43}$ erg. Assuming the loop length and radius are $l = 3 \times 10^6$ cm and $a = 3 \times 10^5$ cm, respectively, we find its inductance $L \approx 5 \times 10^6$ cm $= 5 \times 10^{-3}$ H. Supposing that a significant part of the energy stored in a typical loop ($W \approx 2 \times 10^{43}$ erg $= 2 \times 10^{36}$ J) has been released, we estimate the current $I = (2W/L)^{1/2} \approx 3 \times 10^{19}$ A. From the value of the current we estimate the magnitude of the φ-component of the loop magnetic field: $B_\varphi \approx I/ca \approx 10^{13}$ G. The concentration n of electron–positron pairs in the source is defined by the magnitude of current $I = encS$ and the cross section S of a coronal loop with the radius $a = 3 \times 10^5$ cm. For the current $I = 3 \times 10^{19}$ A, the quantity $n = 2 \times 10^{16}$ cm^{-3}, i.e., the Langmuir frequency $\nu_\mathrm{L} = 1.3 \times 10^{12}$ Hz falls in the terahertz band.

The power of energy release from a typical loop is $\mathrm{d}W/\mathrm{d}t \approx 2 \times 10^{40}$ erg s^{-1} $= 2 \times 10^{33}$ W. The magnitude of a loop resistance in the 'pulsating tail' is $R = (\mathrm{d}W/\mathrm{d}t)\, I^{-2} \approx \approx 2 \times 10^{-6}$ Ω. Such a resistance can be attributed to anomalous conductivity accompanying the excitation of small-scale plasma waves. The minimum (20 Hz) and maximum

(2400 Hz) pulsation frequencies of SGR 1806-20 allow one to estimate the capacitance of magnetic loops carrying the current. As a result, we obtain $C_1 \approx 1.5 \times 10^{-2}$ F and $C_2 \approx 8 \times 10^{-7}$ F, whereas the magnitudes of Q factors for minimum and maximum frequencies are $Q_1 \approx 3 \times 10^5$ and $Q_2 \approx 10^7$. Notice that the magnitude of the magnetic field found in this way, $B \approx 10^{13}$ G, is less than the quantum-electrodynamical threshold $B_{\rm QED} = 4.4 \times 10^{13}$ G at which the nonrelativistic Landau energy $\hbar eB/m_e c$ is comparable to the electron rest mass $m_e c^2$.

8. Conclusion

Natural manifestations of solar and stellar activity — oscillations and waves modulating the emission of the Sun and stars — contain information on coronal parameters, and often it is unique. As a consequence, coronal seismology offers an effective way of diagnosing stellar coronae. The variety of oscillatory and wave processes in solar and stellar coronae is not limited to the cases considered above. In this report, we did not touch on the seismologies of prominences and sunspots, which present separate branches of helioseismology. Further development in methods of coronal seismology is simulated by novel multiwavelength observations of the activity of the Sun and stars. Recent reviews of advances in coronal seismology [29, 38] need to be complemented even now. For instance, fresh SDO observations [39] have revealed manifestations of Kelvin–Helmholtz instability at the boundary of coronal plasma ejection.

This work was supported by RFBR grants 11-02-00103-a, 12-02-00616-a, and 12-02-92703-IND_a, by programs P-21 and P-22 of the Presidium of RAS, and also by Programs of Leading Scientific Schools NSh-1625.2012.2 and NSh-4185.2012.2.

References

1. Kosovichev A G, Duvall T L (Jr.), Scherrer P H *Solar Phys.* **192** 159 (2000)
2. Scherrer P H et al. *Solar Phys.* **275** 207 (2012)
3. Uchida Y *Publ. Astron. Soc. Jpn.* **22** 341 (1970)
4. Rosenberg H *Astron. Astrophys.* **9** 159 (1970)
5. Aschwanden M J et al. *Solar Phys.* **206** 99 (2002)
6. Zaitsev V V, Stepanov A V *Issled. Geomagn., Aeronomii Fiz. Solntsa* (37) 3 (1975)
7. Edwin P M, Roberts B *Solar Phys.* **88** 179 (1983)
8. Meerson B I, Sasorov P V, Stepanov A V *Solar Phys.* **58** 165 (1978)
9. Nakariakov V M, Melnikov V F, Reznikova V E *Astron. Astrophys.* **412** L7 (2003)
10. Nakariakov V M, Ofman L *Astron. Astrophys.* **372** L53 (2001)
11. Kopylova Yu G et al. *Pis'ma Astron. Zh.* **33** 792 (2007) [*Astron. Lett.* **33** 706 (2007)]
12. Tsap Y T et al. *Solar Phys.* **253** 161 (2008)
13. De Moortel I *Space Sci. Rev.* **149** 65 (2009)
14. McIntosh S W et al. *Nature* **475** 477 (2011)
15. Vasheghani Farahani S et al. *Astron. Astrophys.* **498** L29 (2009)
16. Nakariakov V M et al. *Astron. Astrophys.* **452** 343 (2006)
17. Zaitsev V V, Stepanov A V *Pis'ma Astron. Zh.* **8** 248 (1982) [*Sov. Astron. Lett.* **8** 132 (1982)]
18. Zaitsev V V, Stepanov A V *Pis'ma Astron. Zh.* **15** 154 (1989) [*Sov. Astron. Lett.* **15** 66 (1989)]
19. Braginskii S I, in *Voprosy Teorii Plazmy* (Reviews in Plasma Physics) Vol. 1 (Ed. M A Leontovich) (Moscow: Gosatomizdat, 1963) p. 183 [Translated into English (New York: Consultants Bureau, 1965) p. 205]
20. Priest E R *Solar Magneto-hydrodynamics* (Dordrecht: D. Reidel Publ. Co., 1982)
21. Stepanov A V et al. *Pis'ma Astron. Zh.* **31** 684 (2005) [*Astron. Lett.* **31** 612 (2005)]
22. Tsap Yu T et al. *Pis'ma Astron. Zh.* **37** 53 (2011) [*Astron. Lett.* **37** 49 (2011)]
23. Haisch B M, in *Activity in Red-Dwarf Stars*: *Proc. of the 71st Colloquium of the IAU, Catania, Italy, August 10–13, 1982* (Astrophysics and Space Science Library, Vol. 102, Eds P B Byrne, M Rodonò) (Dordrecht: D. Reidel Publ. Co., 1983) p. 255
24. Qin Z et al. *Solar Phys.* **163** 383 (1996)
25. Kopylova Yu G, Stepanov A V, Tsap Yu T *Pis'ma Astron. Zh.* **28** 870 (2002) [*Astron. Lett.* **28** 783 (2002)]
26. Spangler S R *Astrophys. J.* **670** 841 (2007)
27. Severny A *Space Sci. Rev.* **3** 451 (1964)
28. Alfvén H, Carlqvist P *Solar Phys.* **1** 220 (1967)
29. Zaitsev V V, Stepanov A V *Usp. Fiz. Nauk* **178** 1165 (2008) [*Phys. Usp.* **51** 1123 (2008)]
30. Zaitsev V V et al. *Astron. Astrophys.* **337** 887 (1998)
31. Zaitsev V V et al. *Izv. Vyssh. Uchebn. Zaved. Radiofiz.* **54** 243 (2011) [*Radiophys. Quantum Electron.* **54** 219 (2011)]
32. Kislyakova K G et al. *Astron. Zh.* **88** 303 (2011) [*Astron. Rep.* **55** 275 2011)]
33. Landau L D, Lifshitz E M *Mekhanika* (Mechanics) (Moscow: Fizmatgiz, 1958) [Translated into English (Oxford: Pergamon Press, 1960)]
34. Zaitsev V V, Kislyakova K G *Astron. Zh.* **87** 410 (2010) [*Astron. Rep.* **54** 367 (2010)]
35. Terasawa T et al. *Nature* **434** 1110 (2005)
36. Strohmayer T E, Watts A L *Astrophys. J.* **653** 593 (2006)
37. Stepanov A V, Zaitsev V V, Valtaoja E *Pis'ma Astron. Zh.* **37** 303 (2011) [*Astron. Lett.* **37** 276 (2011)]
38. Nakariakov V M, Erdélyi R (Guest Eds) "Solar coronal seismology" *Space Sci. Rev.* **149** (1–4) (2009)
39. Foullon C et al. *Astrophys. J.* **729** L8 (2011)

PACS numbers: **26.60.–c**, **67.10.–j**, 97.60.Jd
DOI: 10.3367/UFNe.0182.201209g.1006

Superfluid neutron stars

P S Shternin, D G Yakovlev

1. Cooling of neutron stars and properties of superdense matter

This talk summarizes the recent interpretation of observations (carried out in 2000–2010 with the NASA's Chandra X-ray orbital observatory) of the young (about 330-year old) neutron star in the Cassiopeia A supernova remnant. The data indicate that the neutron star has a carbon atmosphere and remains warm but shows noticeable cooling, so that its surface temperature has decreased by about 4% in the 10 years of observations. These are the first observations of an isolated neutron star cooling in real time. It is difficult to explain them using the cooling theory for nonsuperfluid neutron stars, but they are naturally explained if the superdense core of the star possesses a strong superfluidity of protons (with a critical temperature higher than 3×10^9 K) and a moderately strong superfluidity of neutrons (with the maximum critical temperature of order $(5-9) \times 10^8$ K over the stellar core). If the observations are correct, these data

P S Shternin, D G Yakovlev Ioffe Physical Technical Institute, Russian Academy of Sciences, St. Petersburg, Russian Federation;
St. Petersburg State Polytechnical University, St. Petersburg, Russian Federation
E-mail: pshternin@gmail.com, yak@astro.ioffe.rssi.ru

Uspekhi Fizicheskikh Nauk **182** (9) 1006–1012 (2012)
DOI: 10.3367/UFNr.0182.201209g.1006
Translated by D G Yakovlev; edited by A Radzig